

Bounding of double-differenced correlated errors of multi-GNSS observations using RTK for AV positioning

Hassan Elsayed and Ahmed El-Mowafy

GNSS-SPAN GROUP,

SCHOOL OF EARTH AND PLANETARY SCIENCES, CURTIN UNIVERSITY, PERTH, AUSTRALIA



Contents

Introduction

Research objective

Methodology

Results

Conclusion

Future work

IM for Autonomous vehicles

- Real-time positioning is key component in Autonomous Vehicles (AV).
- Safety is paramount for AV.
- We need to guarantee the reliability of positioning, i.e. Positioning integrity monitoring (IM).

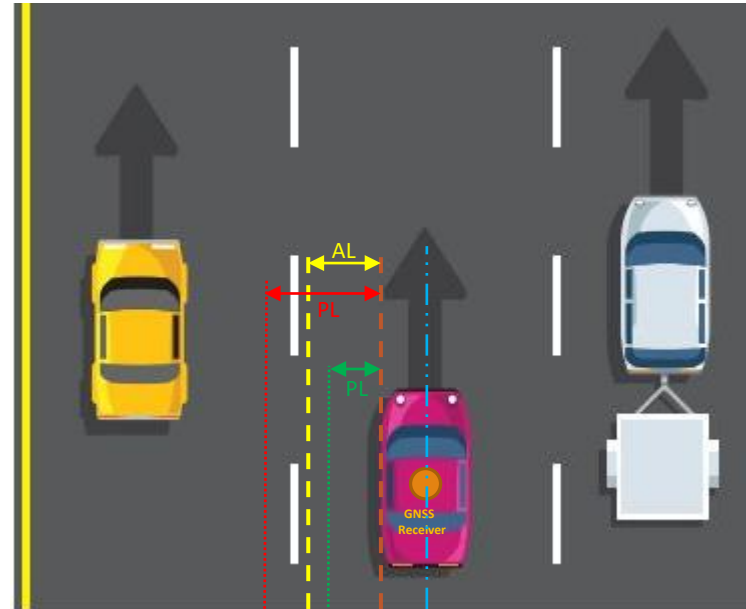


Background: Integrity monitoring

Positioning Integrity Monitoring is about how much trust the user can put in the obtained position.

Integrity definitions:

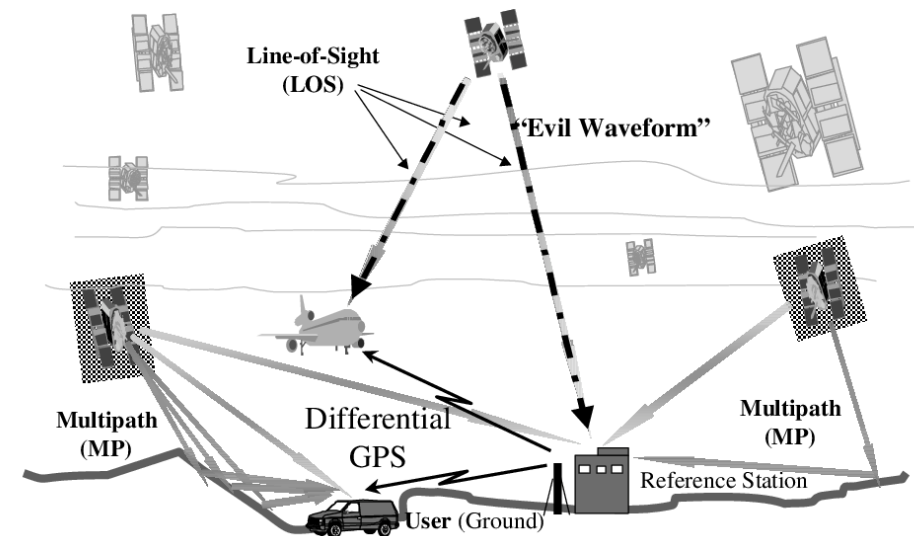
- Alert Limit (AL)
- Protection level (PL)
- Probability of misleading information (P_{HMI})
- Probability of false alert (P_{FA})



ARAIM

- Advanced Receiver Autonomous Integrity Monitoring or ARAIM
- Developed for aviation applications with multi-frequency observations and multi-hypothesis for faults

| Airborne applications | Ground applications |
|----------------------------|---------------------------|
| Smoothed code observations | Phase observations |
| Snapshot positioning | Precise positioning (RTK) |
| Tens of meters accuracy | cm/dm accuracy |



Multicorrelator techniques for robust mitigation of threats to GPS signal quality (R. E. Phelts, 2001)

ARAIM baseline steps and equations

Calculating the all-in-view position $\hat{x}^{(0)}$

$$\Delta\hat{x} = (G^T W G)^{-1} G^T W r$$

$\Delta\hat{x}$ is position solution update at each iteration

Define the threat model with (K) fault modes and calculate the following for each fault mode subset:

- 1) Probability ($P^{(K)}$)
- 2) Position solution ($\hat{x}^{(K)}$)

Commencing FDE

SST

$$T_{k,q} = K_{fa,q} \sigma_{ss,q}^{(K)}$$

$$\tau_{k,q} = \frac{|\hat{x}_q^{(K)} - \hat{x}_q^{(0)}|}{T_{k,q}} \leq 1$$

Chi-square test

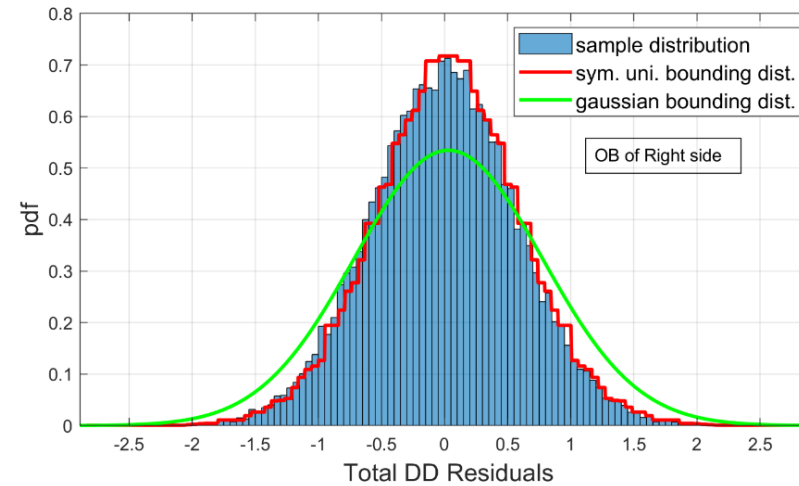
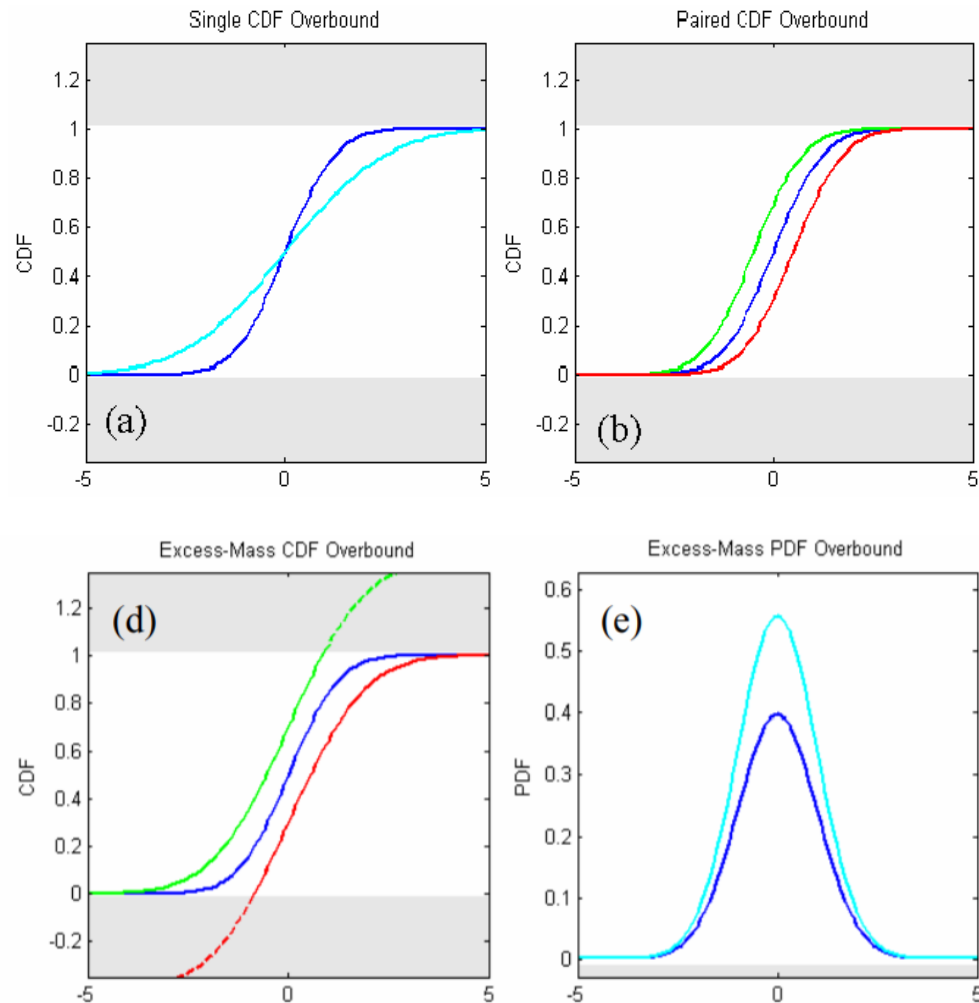
$$\chi^2 = y^T (W - W G (G^T W G)^{-1} G^T W) y$$

$$T_{\chi^2} = (\chi_{deg}^2)^{-1} (1 - P_{FA-Chi^2})$$

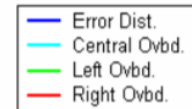
When FDE passes, Commencing PL computation

$$2Q \left[\frac{PL - b_q^{(0)}}{\sigma_q^{(0)}} \right] + \sum_{K=1}^{N_{fault\ modes}} P_{fault,K} Q \left[\frac{PL - T_{K,q} - b_q^{(K)}}{\sigma_q^{(K)}} \right] = \frac{1}{2} PHMI_{Horizontal}$$

Overbounding of the CDF of the error distribution



Overbounding using Two Step Gaussian Bounding Method (TSGB)



Integrity Overview
(Todd Walter, Bruce DeCleene 2015)

Research objective

Building a stochastic model that represents the double-differenced multi-GNSS observations errors for precise positioning of autonomous vehicles utilizing an error bounding technique.

$$\begin{bmatrix}
 \sigma_{G1,2}^2 & q_{G1,2,3} \sigma_{G1,2} \sigma_{G1,3} & q_{G1,2,4} \sigma_{G1,2} \sigma_{G1,4} & 0 & 0 & 0 & 0 & 0 & 0 \\
 q_{G1,2,3} \sigma_{G1,2} \sigma_{G1,3} & \sigma_{G1,3}^2 & q_{G1,3,4} \sigma_{G1,3} \sigma_{G1,4} & 0 & 0 & 0 & 0 & 0 & 0 \\
 q_{G1,2,4} \sigma_{G1,2} \sigma_{G1,4} & q_{G1,3,4} \sigma_{G1,3} \sigma_{G1,4} & \sigma_{G1,4}^2 & 0 & 0 & 0 & 0 & 0 & 0 \\
 0 & 0 & 0 & \sigma_{E1,2}^2 & q_{E1,2,3} \sigma_{E1,2} \sigma_{E1,3} & q_{E1,2,4} \sigma_{E1,2} \sigma_{E1,4} & 0 & 0 & 0 \\
 0 & 0 & 0 & q_{E1,2,3} \sigma_{E1,2} \sigma_{E1,3} & \sigma_{E1,3}^2 & q_{E1,3,4} \sigma_{E1,3} \sigma_{E1,4} & 0 & 0 & 0 \\
 0 & 0 & 0 & q_{E1,2,4} \sigma_{E1,2} \sigma_{E1,4} & q_{E1,3,4} \sigma_{E1,3} \sigma_{E1,4} & \sigma_{E1,4}^2 & 0 & 0 & 0 \\
 0 & 0 & 0 & 0 & 0 & 0 & \sigma_{C1,2}^2 & q_{C1,2,3} \sigma_{C1,2} \sigma_{C1,3} & q_{C1,2,4} \sigma_{C1,2} \sigma_{C1,4} \\
 0 & 0 & 0 & 0 & 0 & 0 & q_{C1,2,3} \sigma_{C1,2} \sigma_{C1,3} & \sigma_{C1,3}^2 & q_{C1,3,4} \sigma_{C1,3} \sigma_{C1,4} \\
 0 & 0 & 0 & 0 & 0 & 0 & q_{C1,2,4} \sigma_{C1,2} \sigma_{C1,4} & q_{C1,3,4} \sigma_{C1,3} \sigma_{C1,4} & \sigma_{C1,4}^2
 \end{bmatrix}$$

A simple example of a variance covariance matrix at one epoch encompassing 12 satellites, i.e. three DD from each constellation.

Collect one
year of RINEX
data from two
Curtin CORS

Compute
Double-
differenced
errors

Mass data
classification,
processing
and analyzing

bounding
using TSGB
method

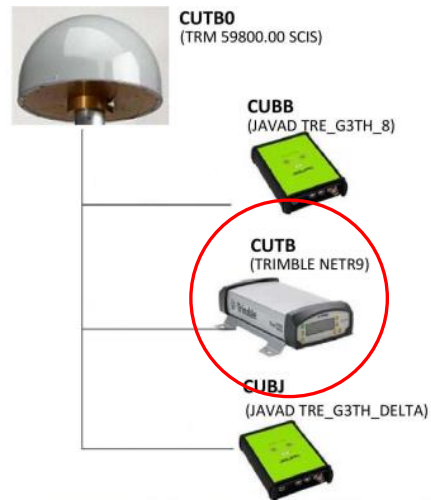
Collect one
year of RINEX
data from two
Curtin CORS

Compute
Double-
differenced
errors

Mass data
classification,
processing
and analyzing

bounding
using TSGB
method

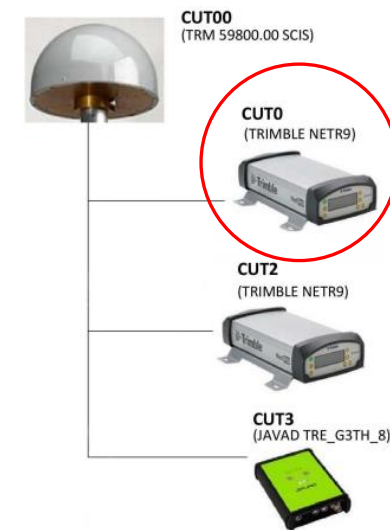
Methodology: Data collection



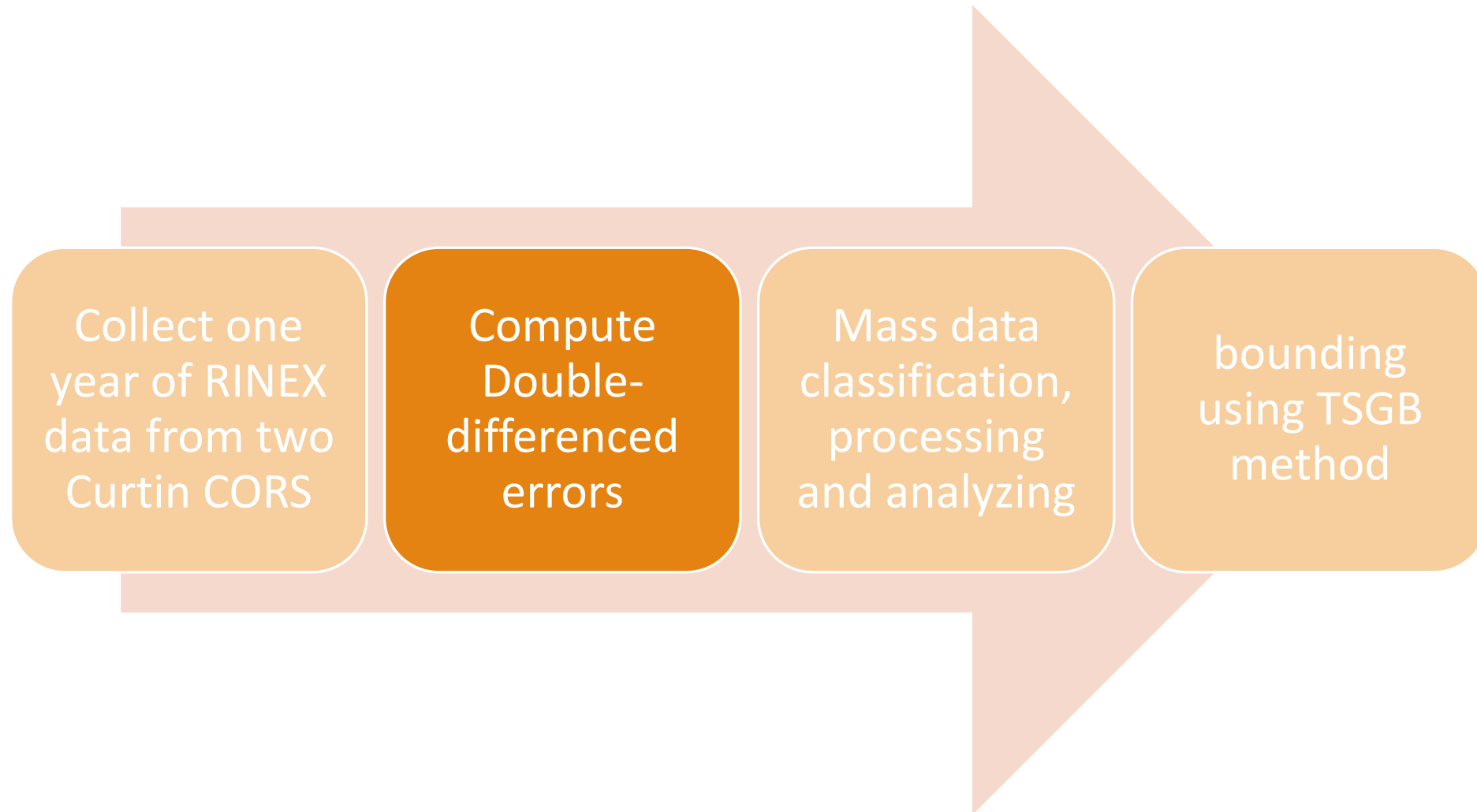
Receivers
configuration
with station
CUTB



Plane view of CORS on top of
building 402 – Curtin
University

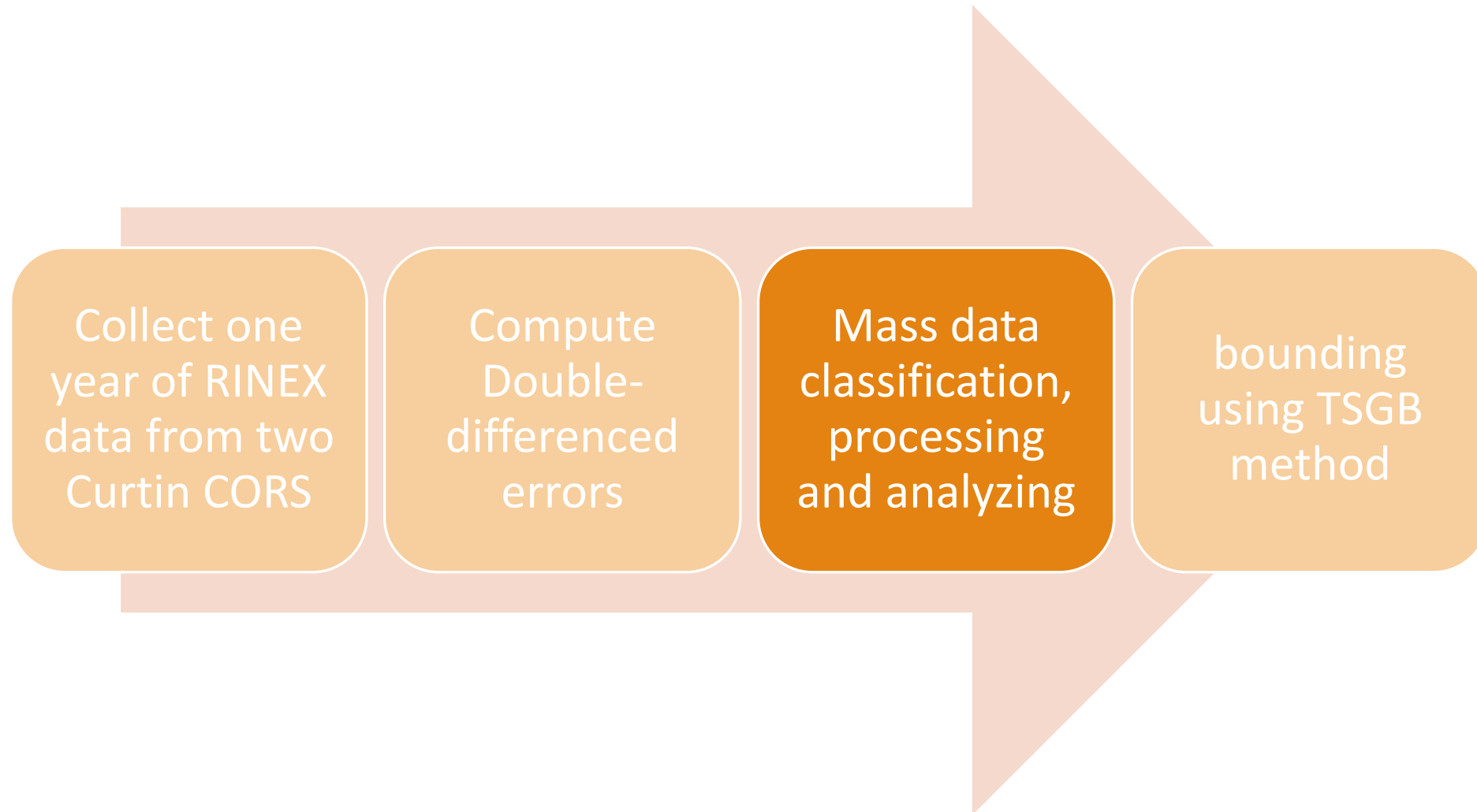


Receivers
configuration
with station
CUT0



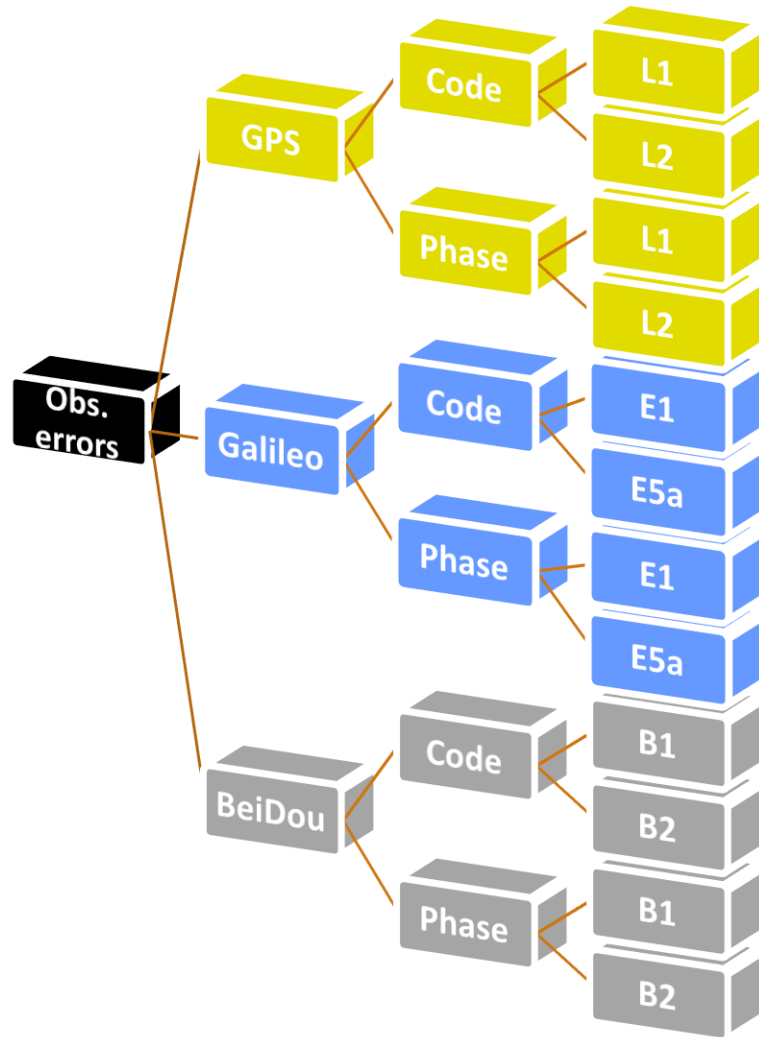
Methodology: Errors extraction

- For phase
$$\varphi_{rb,i}^{jk} = \rho_{rb}^{jk} + \lambda_i (B_{rb,i}^j - B_{rb,i}^k) + \varepsilon_\varphi + b_\varphi$$
- For code
$$P_{rb,i}^{jk} = \rho_{rb}^{jk} + \varepsilon_P + b_P$$
- $\varphi_{rb,i}^{jk}$ and $P_{rb,i}^{jk}$: The DD value of phase and code measurements, respectively for satellites j and k and stations r and b for signal i .
- ρ_{rb}^{jk} : The DD value of the true range between the stations and the satellites.
- λ_i : The wavelength of the observed signal.
- $(B_{rb,i}^j - B_{rb,i}^k)$: The DD value of ambiguity values.
- ε_φ and ε_P : are DD phase and code noise, respectively.
- b_φ and b_P : are DD phase and code biases, respectively.

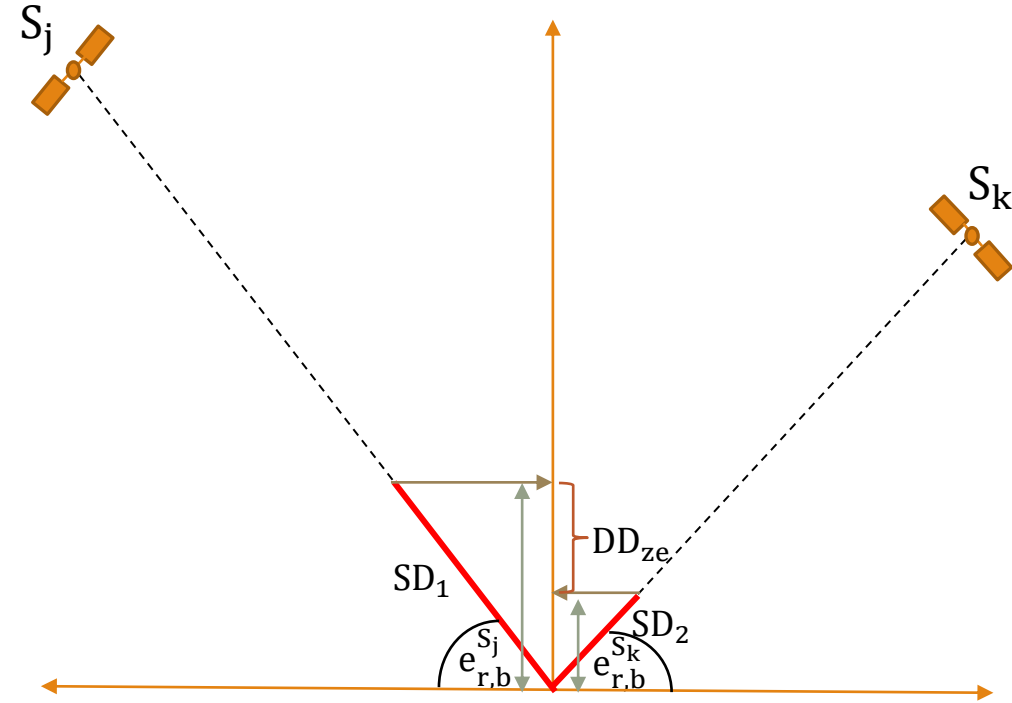


Methodology: Data analysis – 1st empirical method

- Classification:



- Mapping:



$$\begin{aligned} \varepsilon_{rb}^{jk} &= \varepsilon_{rb}^j - \varepsilon_{rb}^k \\ \varepsilon_{rbze}^{jk} &= \varepsilon_{rbze}^j - \varepsilon_{rbze}^k \\ \varepsilon_{rbze}^{jk} &= \varepsilon_{rb}^j f(e_r^{S_j}) - \varepsilon_{rb}^k f(e_b^{S_k}) \end{aligned}$$

Methodology: Data analysis – 1st empirical method

The variance matrix for undifferenced observations at stations r and b :

$$Q_{rb} = \begin{bmatrix} \sigma_0^2 f(e_r^{S_1}) & 0 & 0 & 0 & 0 & 0 & 0 \\ 0 & \sigma_0^2 f(e_b^{S_1}) & 0 & 0 & 0 & 0 & 0 \\ 0 & 0 & \sigma_0^2 f(e_r^{S_2}) & 0 & 0 & 0 & 0 \\ 0 & 0 & 0 & \sigma_0^2 f(e_b^{S_2}) & 0 & 0 & 0 \\ 0 & 0 & 0 & 0 & \ddots & 0 & 0 \\ 0 & 0 & 0 & 0 & 0 & \sigma_0^2 f(e_r^{S_n}) & 0 \\ 0 & 0 & 0 & 0 & 0 & 0 & \sigma_0^2 f(e_b^{S_n}) \end{bmatrix}$$

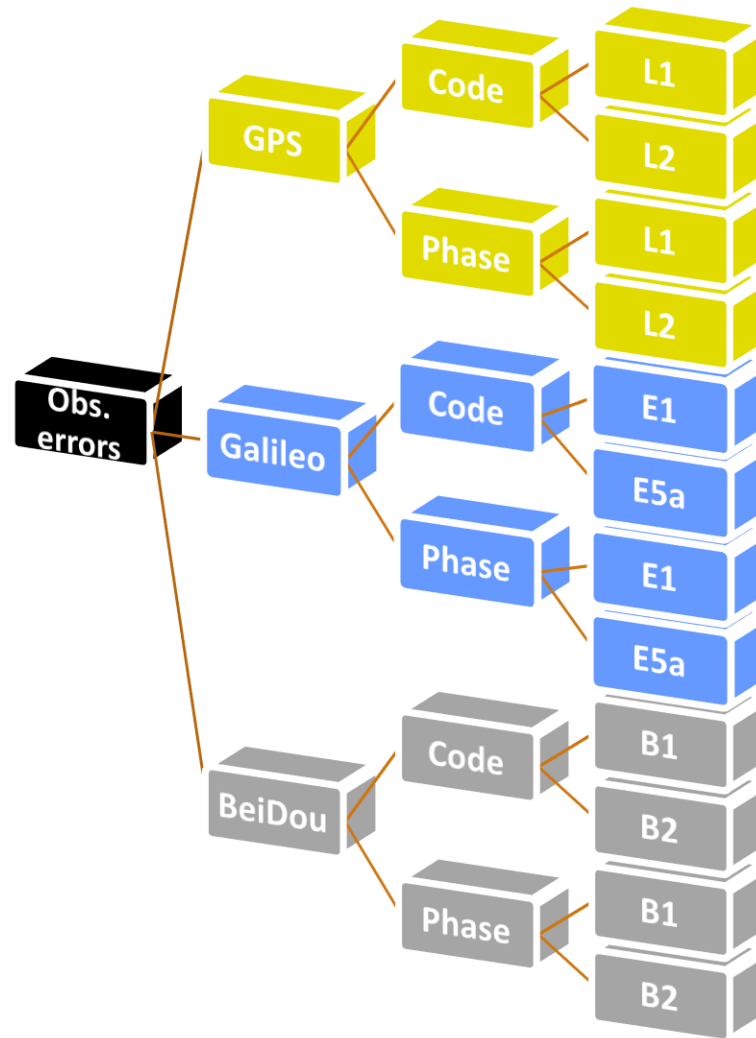
$f(e_r^{S_n})$ and $f(e_b^{S_n})$ are the mapping function dependent on EA $e_r^{S_n}$ or $e_b^{S_n}$, for satellites s_1 to s_n .

The VC matrix for DD observations: $Q_{DD} = A(Q_{rb})A^T$

The correlation coefficient between DD observations:

$$q_{ij} = \frac{f(e_r^{S_1}) + f(e_b^{S_1})}{\sqrt{(f(e_r^{S_1}) + f(e_b^{S_1}) + f(e_r^{S_i}) + f(e_b^{S_i})) \times (f(e_r^{S_1}) + f(e_b^{S_1}) + f(e_r^{S_j}) + f(e_b^{S_j}))}}$$

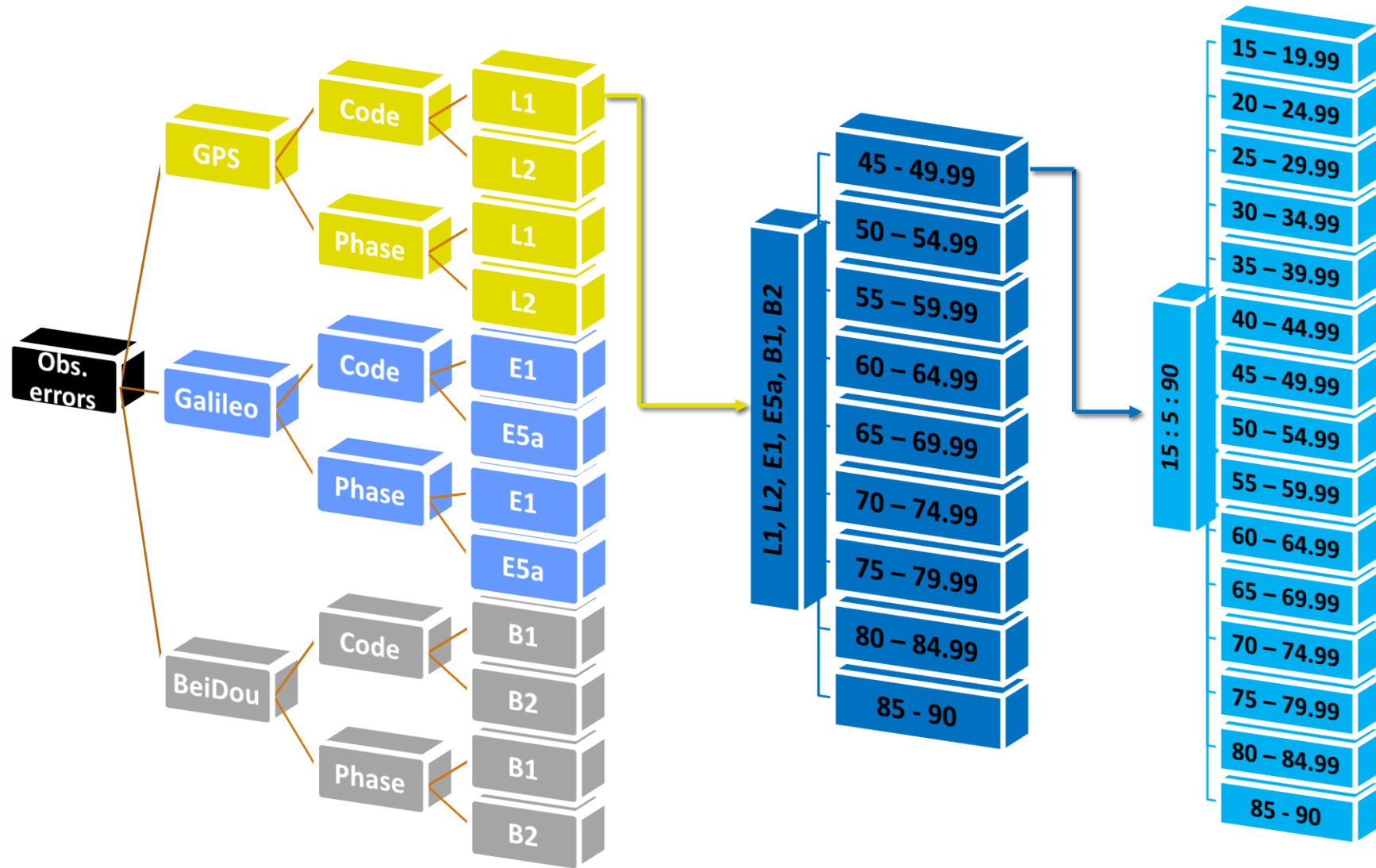
Methodology: Data analysis – 2nd empirical method



Each group of the frequencies' categories is then sorted into 9 groups based on the elevation angle of the pivot satellite with an interval of five degrees.

Each group of the pivot satellite's categories is then sorted into 15 groups based on the elevation angle of the secondary satellite with an interval of five degrees.

Methodology: Data analysis – 2nd empirical method

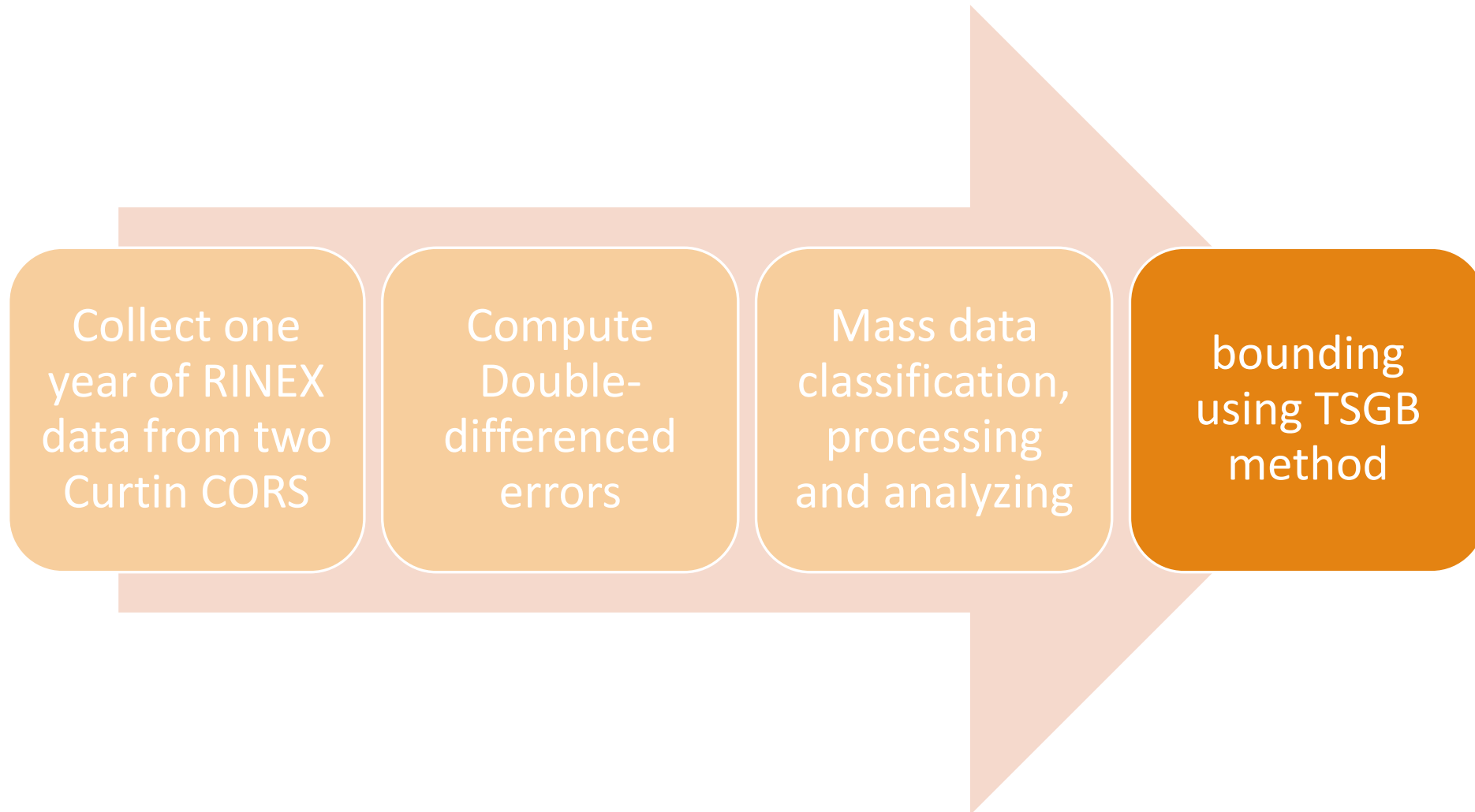


Methodology: Data analysis – 2nd empirical method

The correlation coefficient was calculated between each category using Pearson's Correlation Coefficient:

$$r_{ij} = \frac{n(\sum \varepsilon_i \varepsilon_j) - (\sum \varepsilon_i)(\sum \varepsilon_j)}{\sqrt{[n \sum \varepsilon_i^2 - (\sum \varepsilon_i)^2] [n \sum \varepsilon_j^2 - (\sum \varepsilon_j)^2]}}$$

where i and j are the correlated categories and n is the number of data in a certain category.

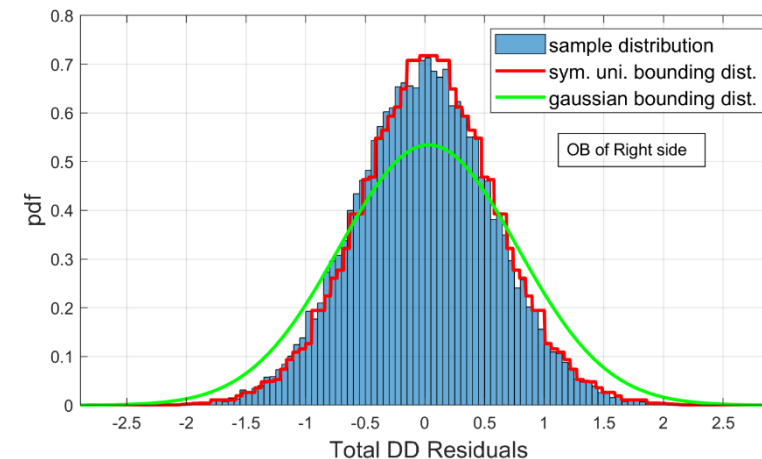
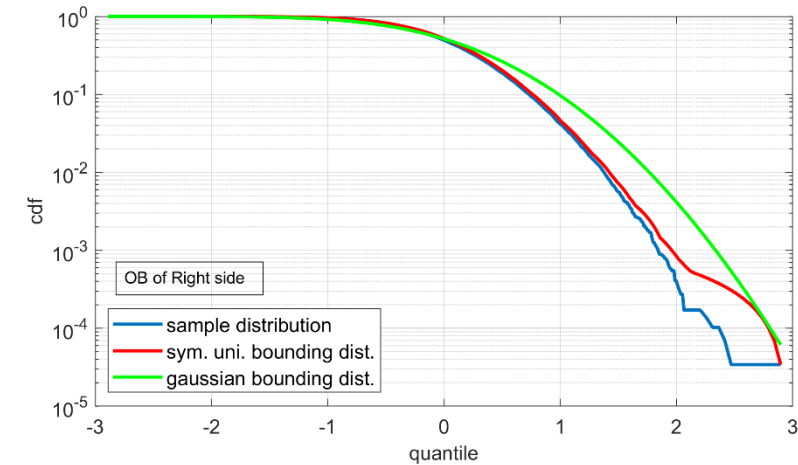


Methodology: TSGB implementation

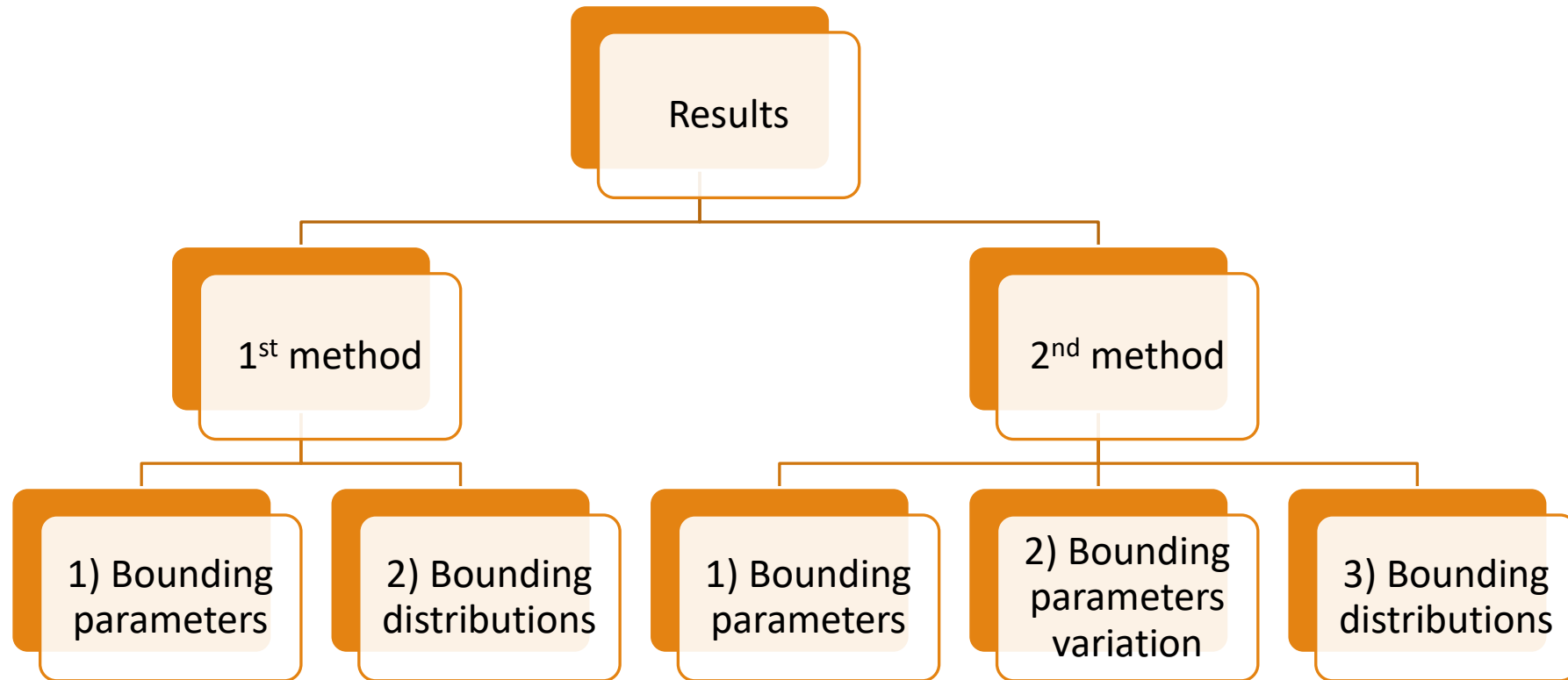
- Forming a symmetric and unimodal distribution.
- performed from both sides of the data and the mean of each half is computed.
- The second step is to find a standard deviation of a Gaussian distribution for each half that achieves the bounding status.

$$F(x) \leq F_S(x) \quad \text{for any } x$$

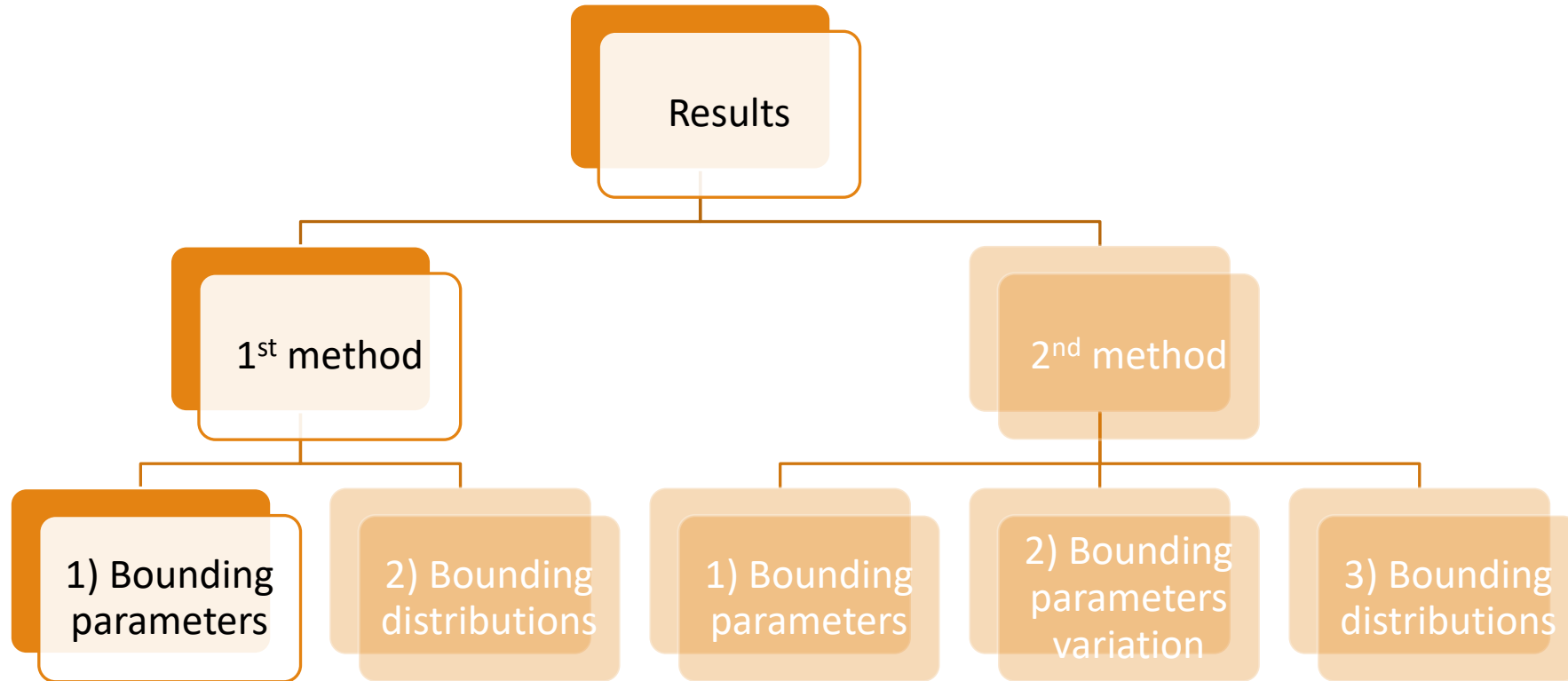
$$F_S(x) \leq \frac{1}{\sqrt{2\pi}} \int_{x-m}^{+\infty} e^{-\frac{t^2}{2\sigma^2}} dt \quad \text{for any } x \geq m$$



Overbounding using Two Step
Gaussian Bounding Method (TSGB)



Results: Bounding parameters of the 1st method

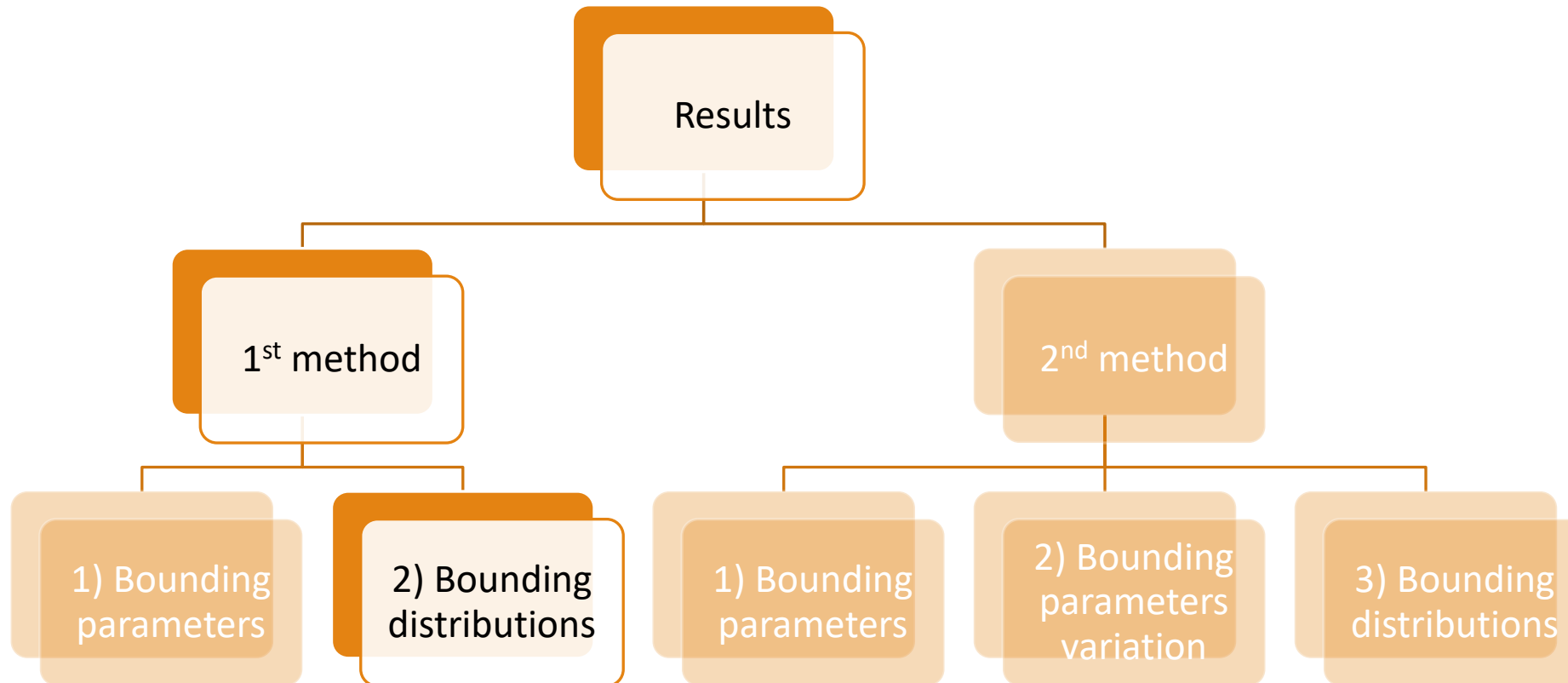


Results: Bounding parameters of the 1st method

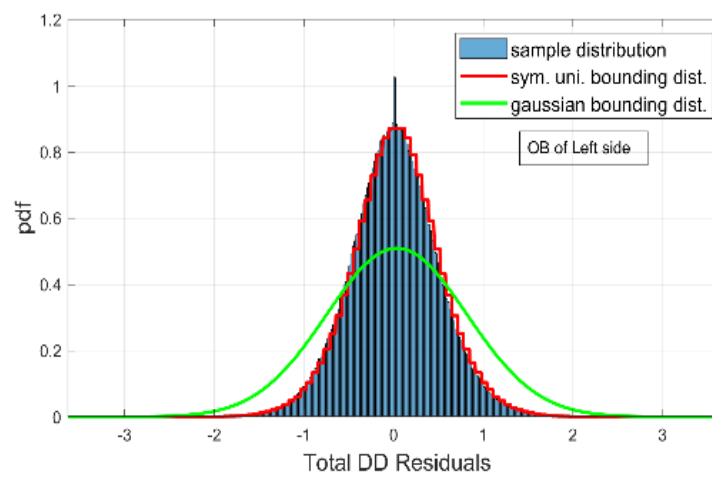
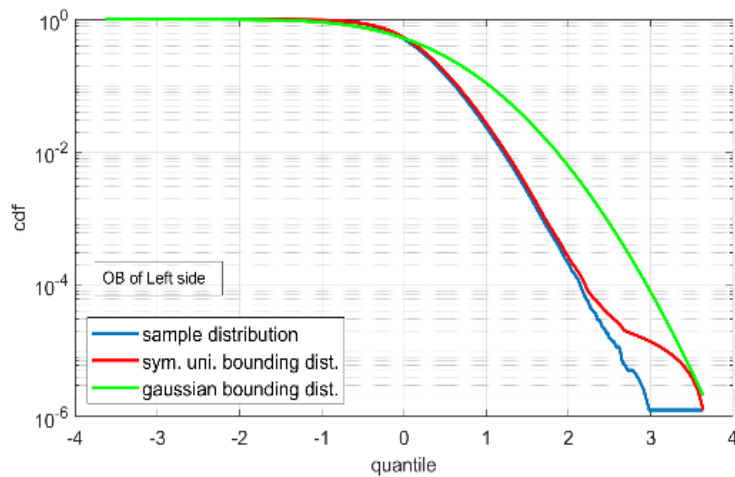
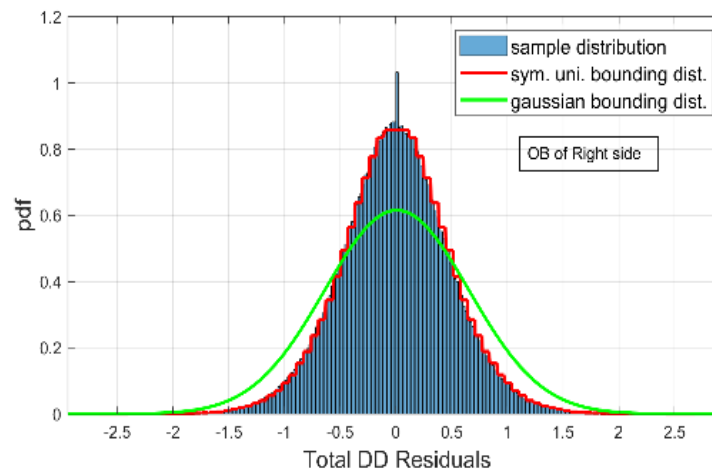
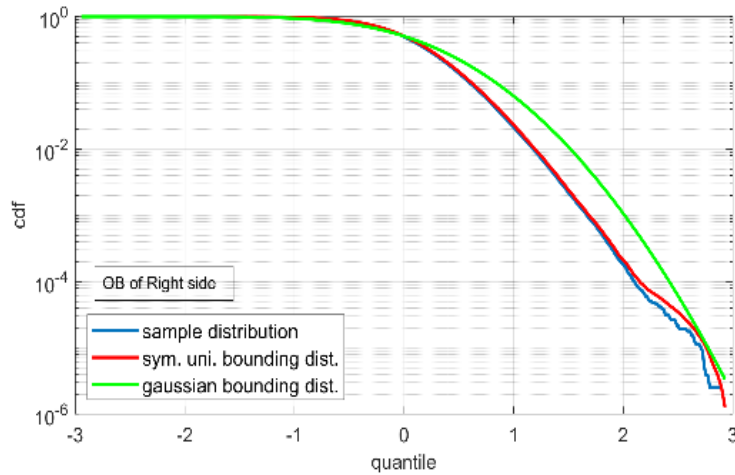
Bounding parameters at zenith of the three investigated systems at different signals and frequencies

| System | Signal | Frequency | Mean (m) | Standard Deviation (m) |
|---------|--------|-----------|----------|------------------------|
| GPS | Code | L1 | 0.03588 | 0.78321 |
| | | L2 | 0.03484 | 0.72368 |
| | Phase | L1 | 0.00032 | 0.01381 |
| | | L2 | 0.00049 | 0.01345 |
| Galileo | Code | E1 | 0.01254 | 0.45621 |
| | | E5a | 0.01711 | 0.34738 |
| | Phase | E1 | 0.00054 | 0.01291 |
| | | E5a | 0.00054 | 0.01242 |
| BeiDou | Code | B1 | 0.02508 | 0.69540 |
| | | B2 | 0.13323 | 0.42987 |
| | Phase | B1 | 0.00171 | 0.01419 |
| | | B2 | 0.00257 | 0.01406 |

Results: Bounding distributions of the 1st method

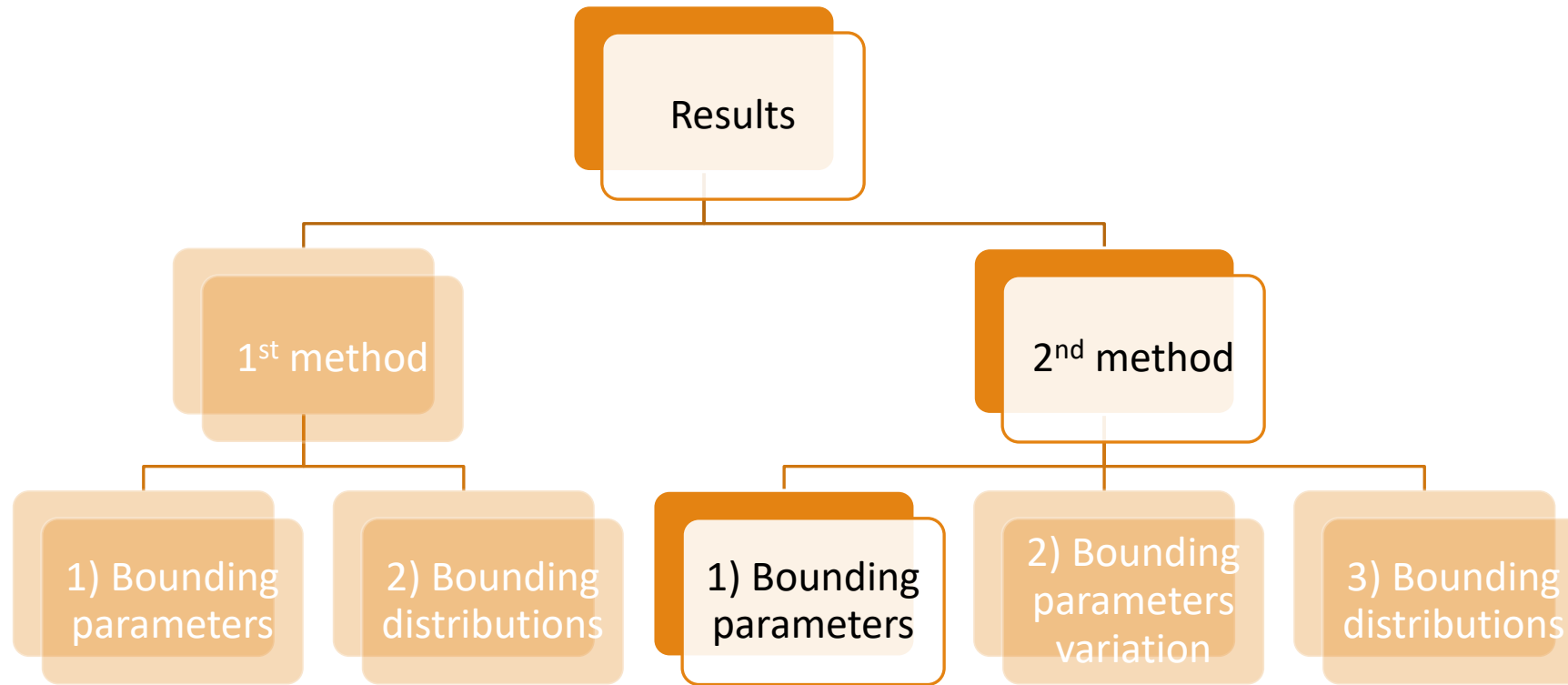


Results: Bounding distributions of the 1st method



Two-step bounding for the GPS L1 DD errors mapped to zenith. The figure shows on the right the actual data distribution, the symmetric unimodal distribution, and the final Gaussian distribution, and on the left their CDFs

Results: Bounding parameters of the 2nd method



Results: Bounding parameters of the 2nd method

| BeiDou - code B1 | | | | | | | | | |
|------------------|-------------------|----|----|---------|---------|---------|---------|---------|---------|
| OB parameters | Bias (error Mean) | | | | | | | | |
| Pivot EA | 45 | 50 | 55 | 60 | 65 | 70 | 75 | 80 | 85 |
| Secondary EA | 45 | 50 | 55 | 60 | 65 | 70 | 75 | 80 | 85 |
| 15 | | | | 0.19466 | 0.26285 | 0.32266 | 0.29991 | 0.23170 | 0.40755 |
| 20 | | | | 0.18686 | 0.10546 | 0.11396 | 0.11536 | 0.14736 | 0.55807 |
| 25 | | | | 0.10507 | 0.06350 | 0.05802 | 0.15963 | 0.14006 | 0.27170 |
| 30 | | | | 0.30927 | 0.28260 | 0.23619 | 0.21581 | 0.14710 | 0.48908 |
| 35 | | | | 0.36730 | 0.16947 | 0.09088 | 0.07114 | 0.05901 | 1.02202 |
| 40 | | | | 0.08993 | 0.16974 | 0.23970 | 0.32063 | 0.19173 | 0.27930 |
| 45 | | | | 0.21434 | 0.09569 | 0.07527 | 0.10195 | 0.05343 | |
| 50 | | | | 0.03522 | 0.07254 | 0.04934 | 0.13634 | 0.14650 | 0.21802 |
| 55 | | | | 0.08351 | 0.03394 | 0.04740 | 0.03993 | 0.05372 | 0.32398 |
| 60 | | | | 0.09527 | 0.03196 | 0.04228 | 0.05351 | 0.04640 | 0.68766 |
| 65 | | | | | 0.07643 | 0.04163 | 0.08280 | 0.09344 | 0.36900 |
| 70 | | | | | | 0.06013 | 1.16393 | 0.04287 | |
| 75 | | | | | | | 0.11879 | 0.03069 | |
| 80 | | | | | | | | | |
| 85 | | | | | | | | | |

Bounding *mean* of data collected at different EAs of the reference and the secondary satellites.

BeiDou code B1 data

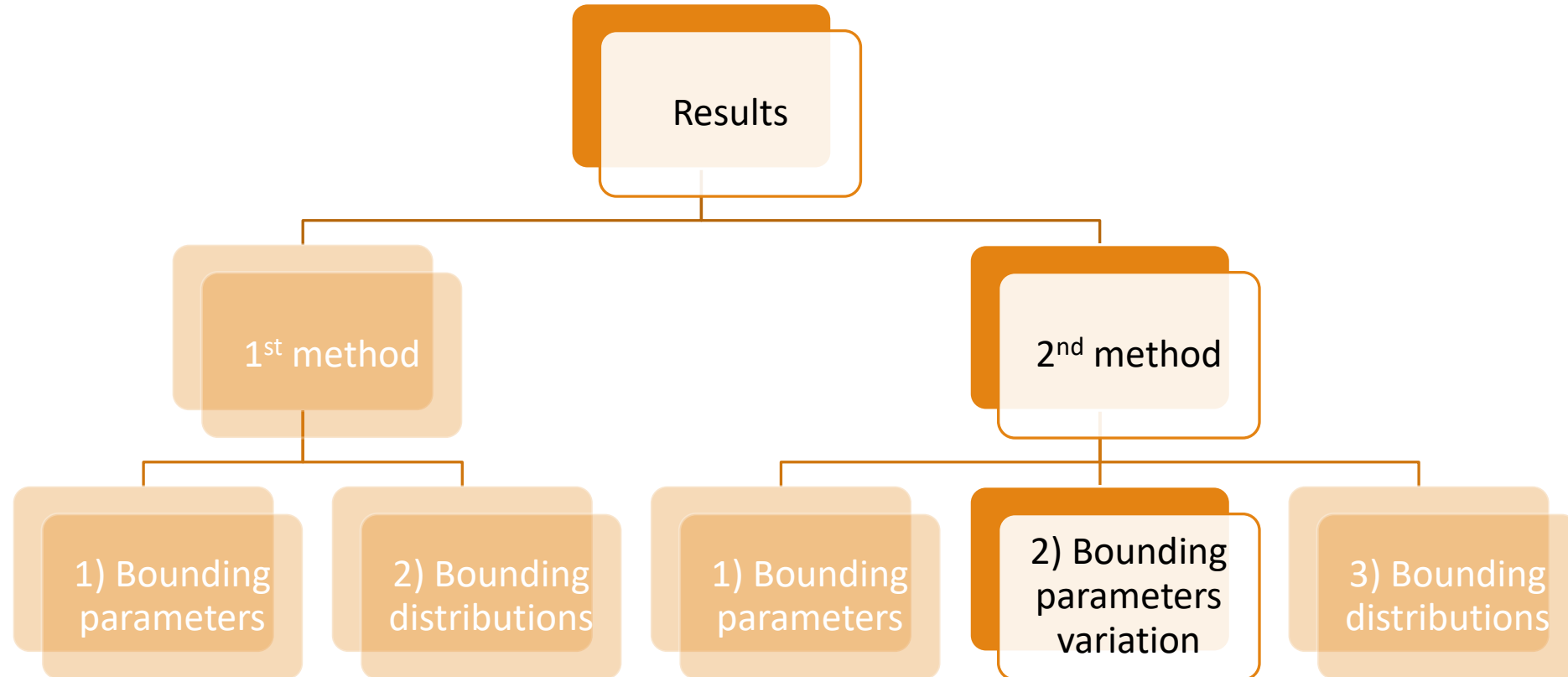
Results: Bounding parameters of the 2nd method

| OB parameters | Standard deviation | | | | | | | | |
|---------------|--------------------|----|----|---------|---------|---------|---------|---------|---------|
| Pivot EA | 45 | 50 | 55 | 60 | 65 | 70 | 75 | 80 | 85 |
| Secondary EA | | | | | | | | | |
| 15 | | | | 1.26271 | 1.58852 | 2.32259 | 2.49742 | 1.27451 | 1.27737 |
| 20 | | | | 1.15377 | 1.06690 | 1.34817 | 1.29533 | 1.11054 | 1.28488 |
| 25 | | | | 1.15291 | 1.07174 | 1.05592 | 1.06467 | 1.05496 | 1.02945 |
| 30 | | | | 0.89072 | 0.98765 | 0.90792 | 0.91941 | 1.06465 | 1.20275 |
| 35 | | | | 0.98070 | 1.04903 | 0.97389 | 1.27317 | 1.12253 | 1.21600 |
| 40 | | | | 1.00239 | 1.10752 | 1.16926 | 1.14126 | 1.06088 | 1.09598 |
| 45 | | | | 1.11023 | 1.06245 | 0.94887 | 1.01617 | 0.94328 | |
| 50 | | | | 0.80934 | 0.72393 | 0.74070 | 0.72991 | 0.84436 | 0.77159 |
| 55 | | | | 0.67239 | 0.74650 | 0.62601 | 0.62805 | 0.60672 | 0.67492 |
| 60 | | | | 0.68487 | 0.64432 | 0.65048 | 0.74803 | 0.62477 | 0.74399 |
| 65 | | | | | 0.59777 | 0.60996 | 0.65351 | 0.64201 | 0.63855 |
| 70 | | | | | | 0.65612 | 0.61696 | 0.56838 | |
| 75 | | | | | | | 0.60486 | 0.57032 | |
| 80 | | | | | | | | | |
| 85 | | | | | | | | | |

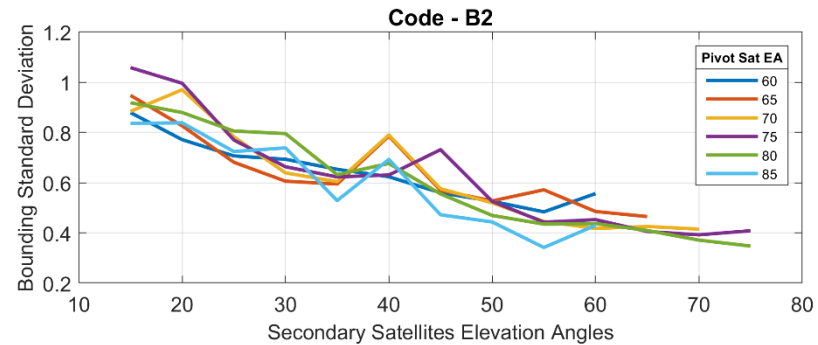
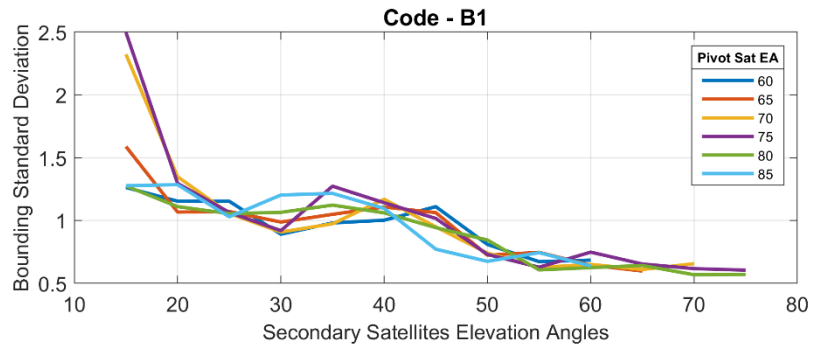
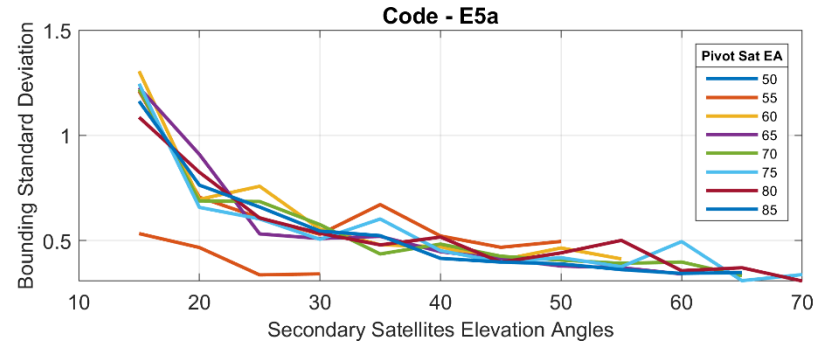
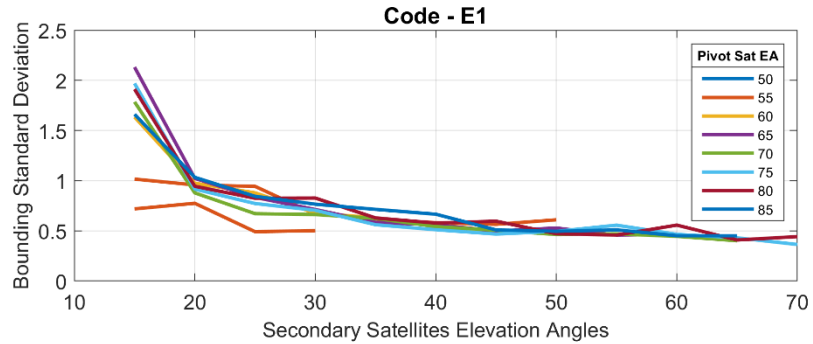
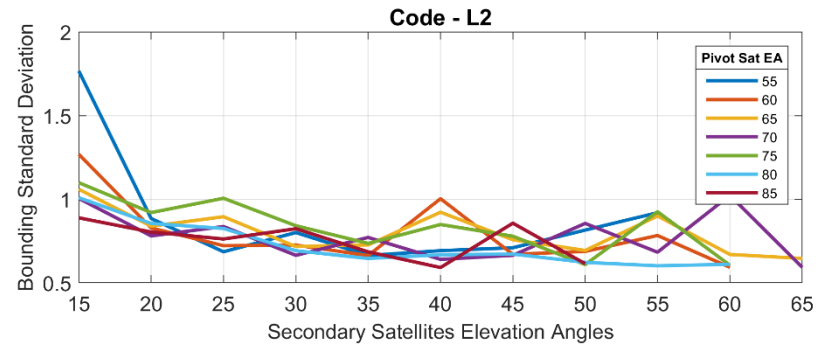
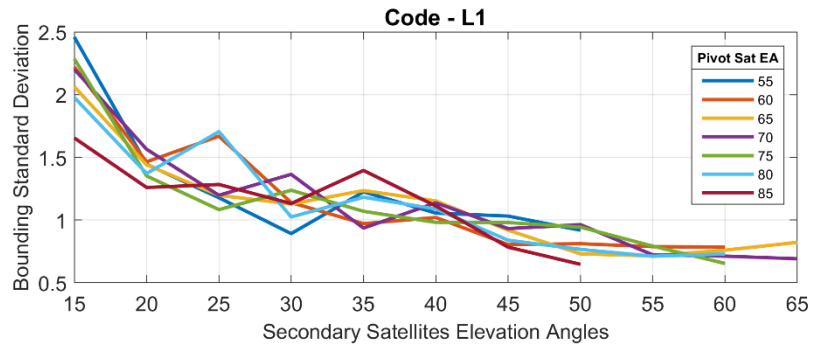
Bounding ***standard deviation*** of data collected at different EAs of the reference and the secondary satellites.

BeiDou code B1 data

Results: Variation of bounding parameters of the 2nd method

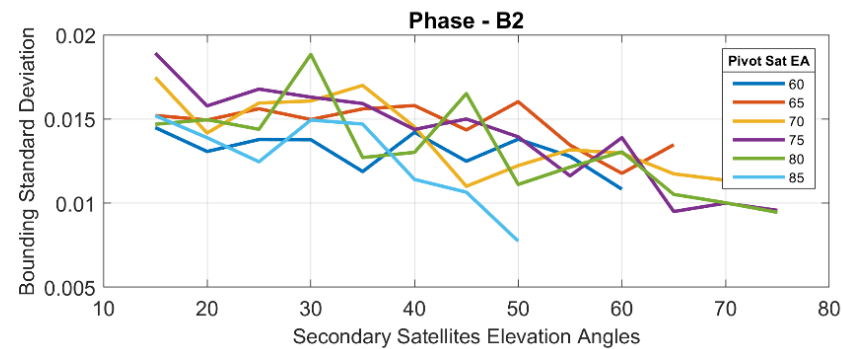
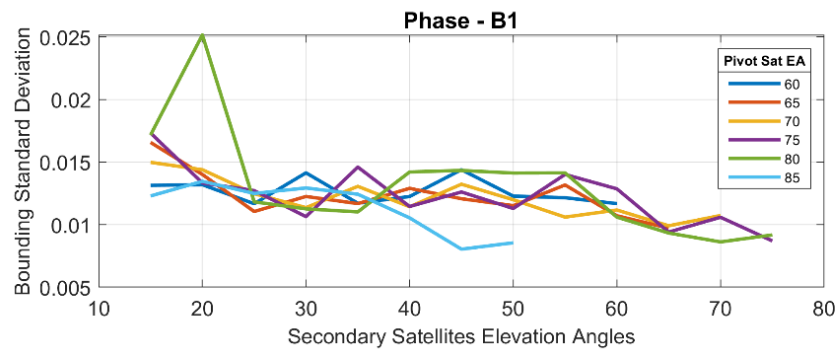
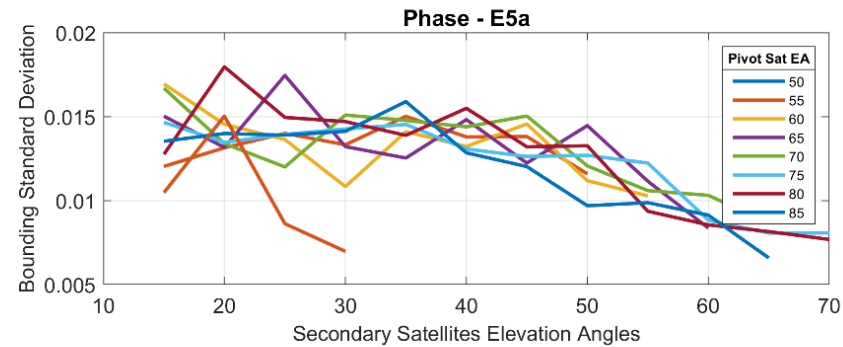
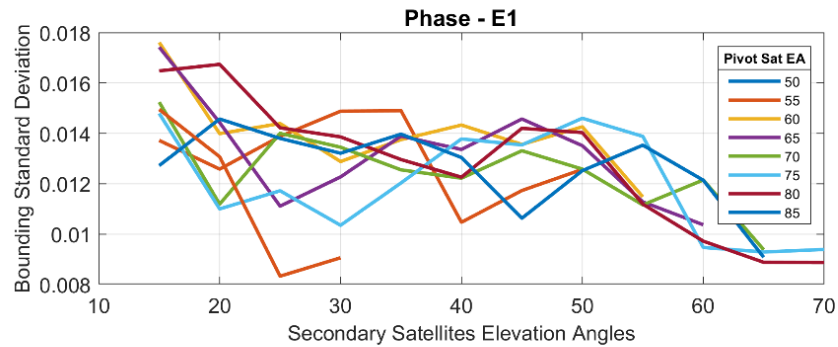
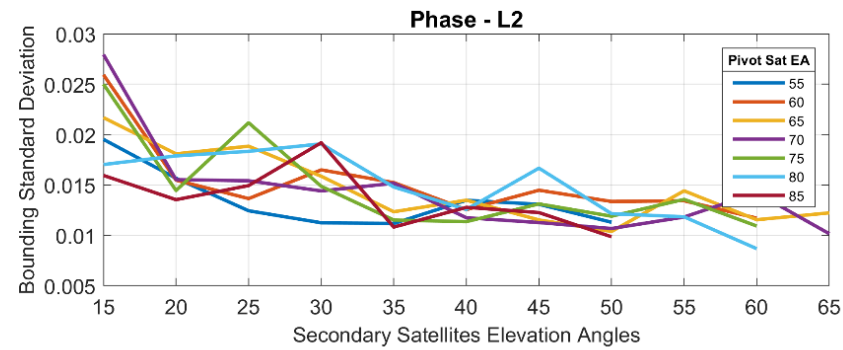
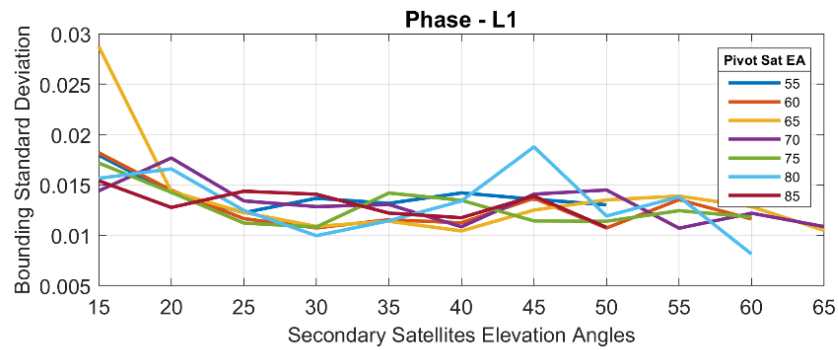


Results: Variation of bounding parameters of the 2nd method



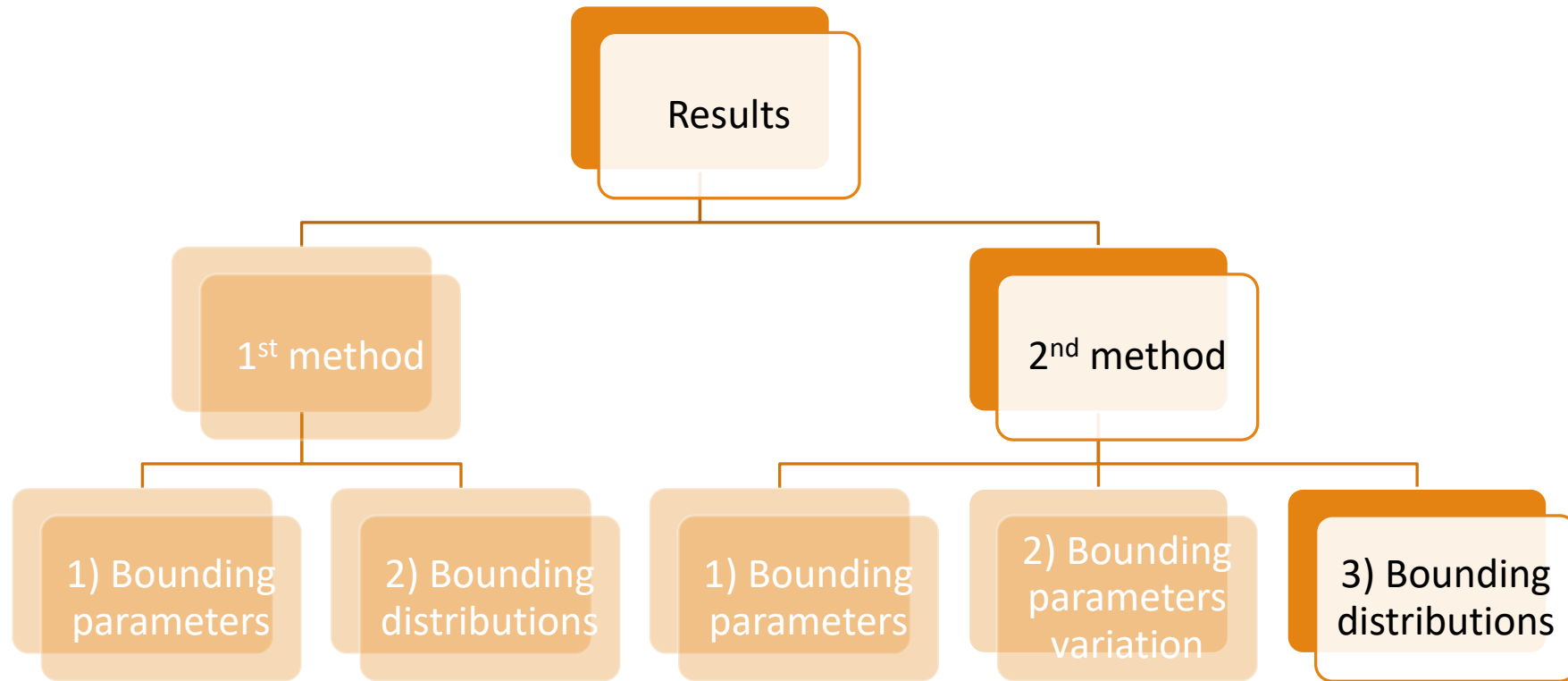
Variation of the bounding standard deviation of the DD *code* errors with respect to the EA of the observed satellites

Results: Variation of bounding parameters of the 2nd method

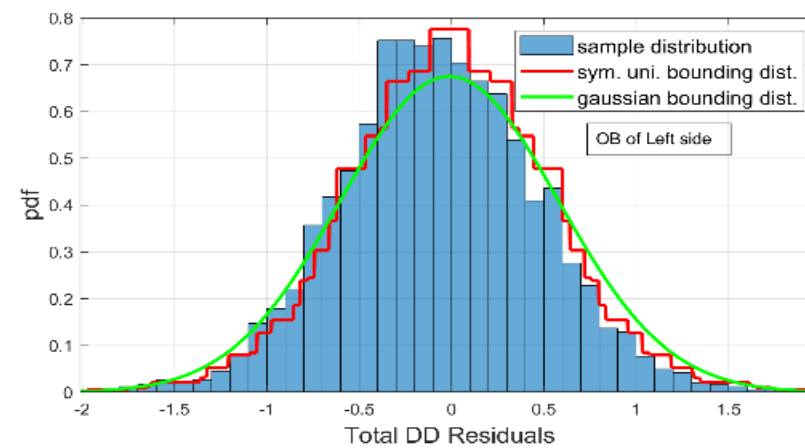
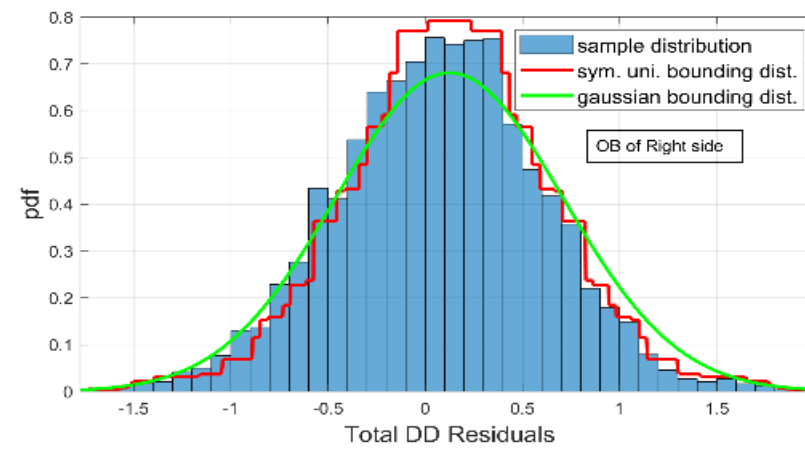
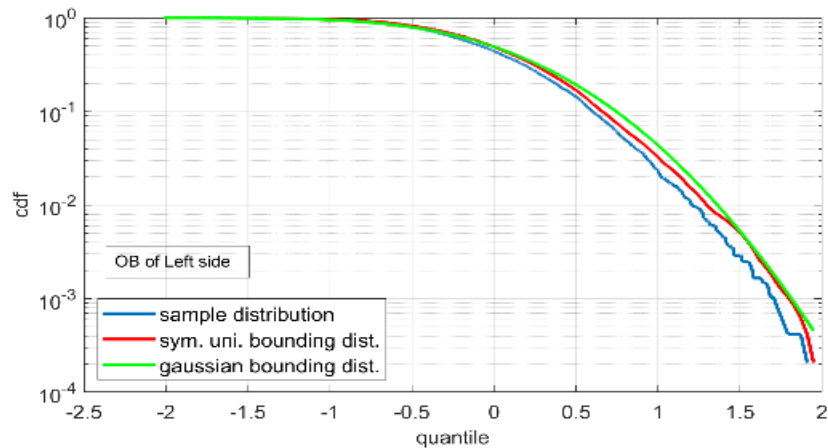
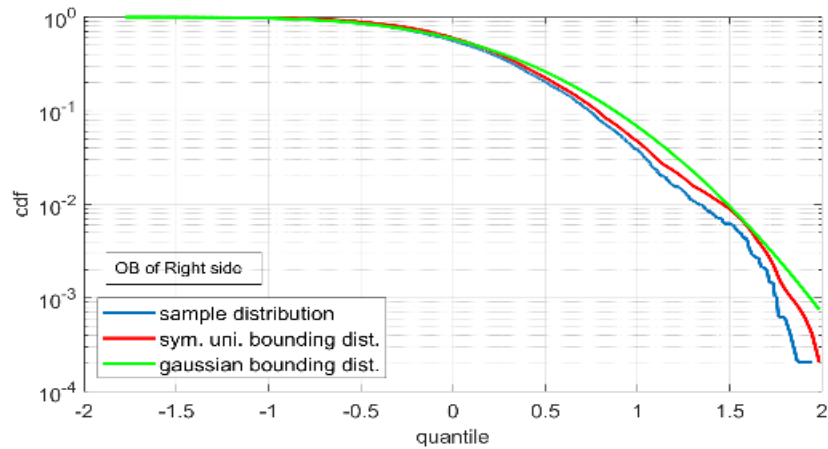


Variation of the bounding standard deviation of the DD *phase* errors with respect to the EA of the observed satellites

Results: Bounding distributions of the 2nd method



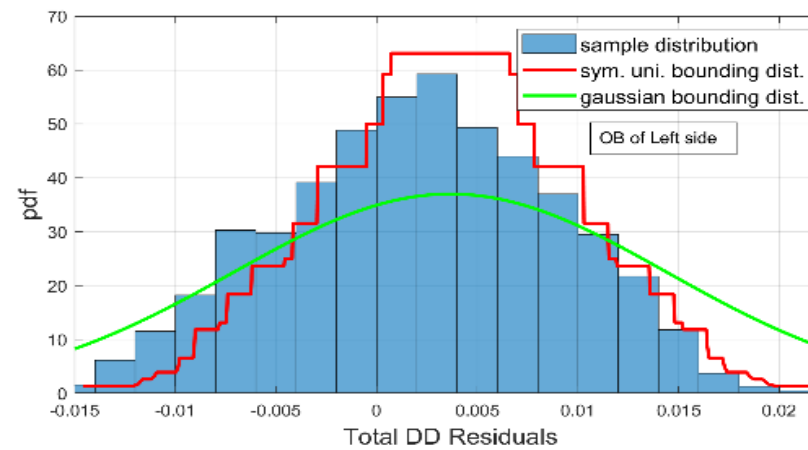
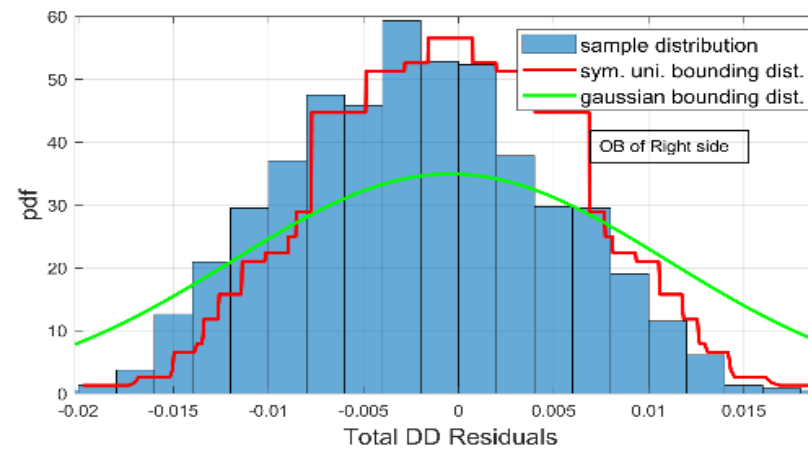
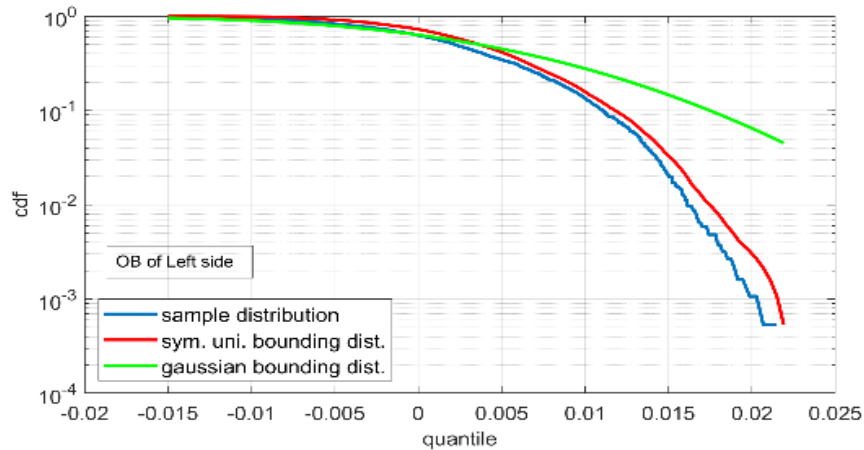
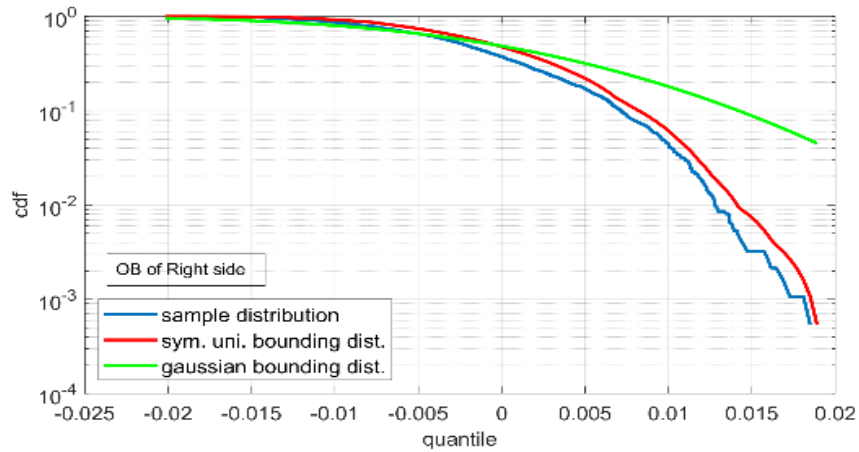
Results: Bounding distributions of the 2nd method



Two-step bounding for the GPS L2 DD code errors collected at 85 and 45 degrees as an EA for the pivot and secondary satellites respectively.

It shows the actual data distribution, the symmetric unimodal distribution, and the final Gaussian distribution (right), and CDFs (left)

Results: Bounding distributions of the 2nd method

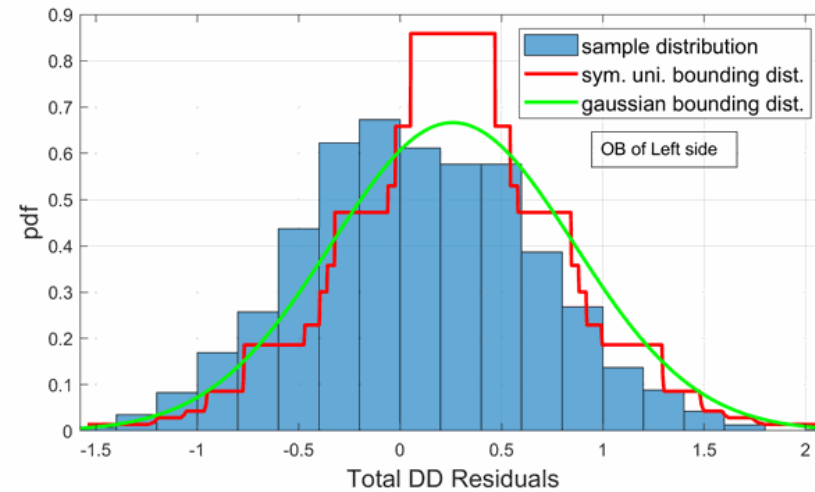
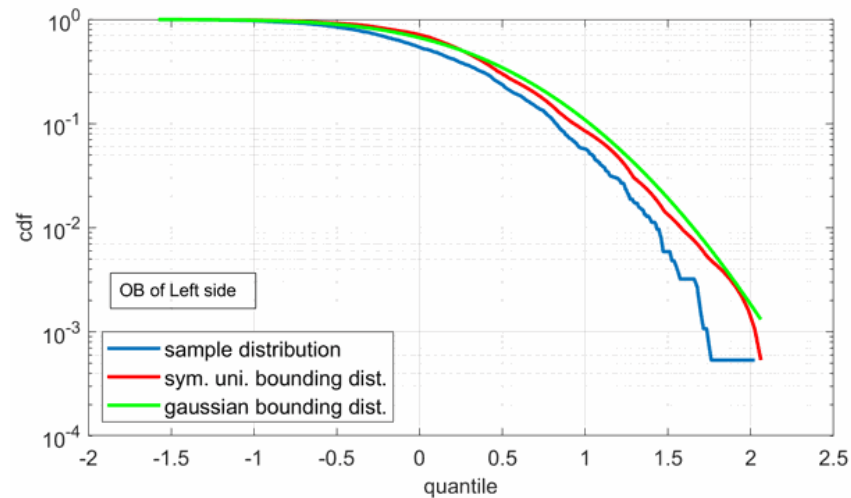
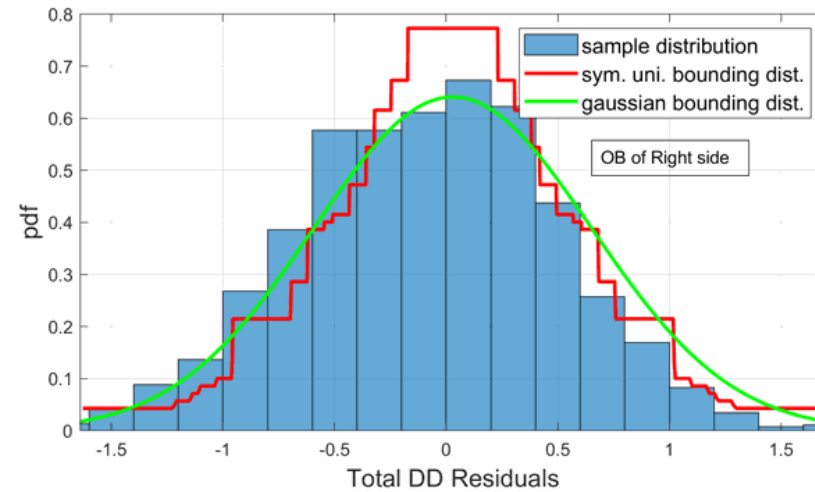
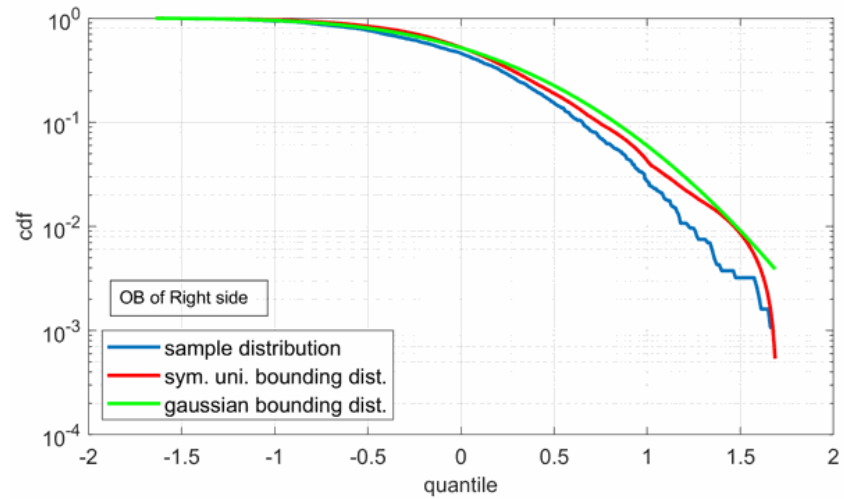


Two-step bounding for the Galileo E1 DD phase errors collected at 45 and 30 degrees as an EA for the pivot and secondary satellites respectively.

It shows the actual data distribution, the symmetric unimodal distribution, and the final Gaussian distribution (right), and CDFs (left)

Results: Bounding distributions of the 2nd method

Overbounding of Galileo DD errors of code measurements for E1 at 45 and 30 degrees as elevation angles for pivot and secondary satellites



Conclusion

This research has proven the possibility to obtain a representative stochastic model that accounts for observations correlation based on empirical data of a relatively short period (one year) using a bounding technique. This weighting function can be used for IM of multi-GNSS precise positioning for autonomous vehicles.

$$\begin{bmatrix}
 \sigma_{G1,2}^2 & q_{G1,2,3} \sigma_{G1,2} \sigma_{G1,3} & q_{G1,2,4} \sigma_{G1,2} \sigma_{G1,4} & 0 & 0 & 0 & 0 & 0 & 0 \\
 q_{G1,2,3} \sigma_{G1,2} \sigma_{G1,3} & \sigma_{G1,3}^2 & q_{G1,3,4} \sigma_{G1,3} \sigma_{G1,4} & 0 & 0 & 0 & 0 & 0 & 0 \\
 q_{G1,2,4} \sigma_{G1,2} \sigma_{G1,4} & q_{G1,3,4} \sigma_{G1,3} \sigma_{G1,4} & \sigma_{G1,4}^2 & 0 & 0 & 0 & 0 & 0 & 0 \\
 0 & 0 & 0 & \sigma_{E1,2}^2 & q_{E1,2,3} \sigma_{E1,2} \sigma_{E1,3} & q_{E1,2,4} \sigma_{E1,2} \sigma_{E1,4} & 0 & 0 & 0 \\
 0 & 0 & 0 & q_{E1,2,3} \sigma_{E1,2} \sigma_{E1,3} & \sigma_{E1,3}^2 & q_{E1,3,4} \sigma_{E1,3} \sigma_{E1,4} & 0 & 0 & 0 \\
 0 & 0 & 0 & q_{E1,2,4} \sigma_{E1,2} \sigma_{E1,4} & q_{E1,3,4} \sigma_{E1,3} \sigma_{E1,4} & \sigma_{E1,4}^2 & 0 & 0 & 0 \\
 0 & 0 & 0 & 0 & 0 & 0 & \sigma_{C1,2}^2 & q_{C1,2,3} \sigma_{C1,2} \sigma_{C1,3} & q_{C1,2,4} \sigma_{C1,2} \sigma_{C1,4} \\
 0 & 0 & 0 & 0 & 0 & 0 & q_{C1,2,3} \sigma_{C1,2} \sigma_{C1,3} & \sigma_{C1,3}^2 & q_{C1,3,4} \sigma_{C1,3} \sigma_{C1,4} \\
 0 & 0 & 0 & 0 & 0 & 0 & q_{C1,2,4} \sigma_{C1,2} \sigma_{C1,4} & q_{C1,3,4} \sigma_{C1,3} \sigma_{C1,4} & \sigma_{C1,4}^2
 \end{bmatrix}$$

Future work

- Investigating the efficiency of the designed empirical weighting functions.
- Carrying out sensitivity analysis to examine different mapping functions or analysing longer periods of GNSS observations.
- Using adaptive Kalman Filter in the FDE step.
- Testing the developed methods by GNSS data collected by low-cost receivers.

Questions?

QUESTIONS

